

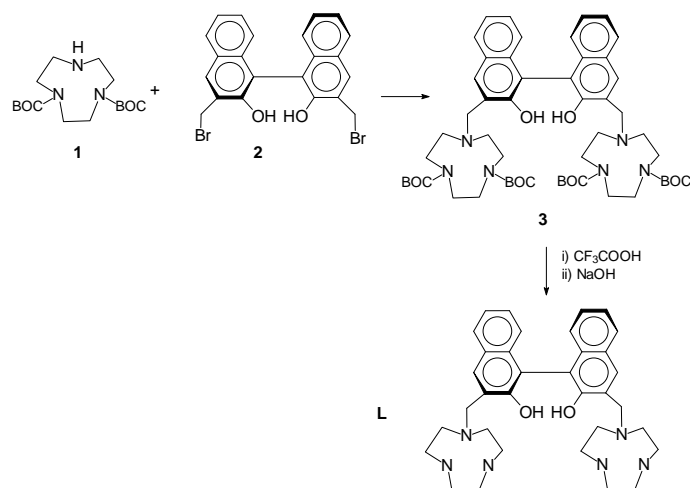
Electronic Supporting Information

Synthesis of the receptor.

Receptor **L** was prepared as sketched in Scheme S1. Reaction of 1,4,7-triazacyclononane-1,4-dicarboxylic acid di-*tert*-butyl ester¹ **1** with (*S*)-(-)-3,3'-bis(bromomethyl)-2,2'-dihydroxy-1,1'-binaphthyl² **2** affords the BOC-protected L derivative **3**, which was subsequently deprotected with CF₃CO₂H.

Synthesis of (BOC)₄-L. To a solution of 1,4,7-triazacyclononane-1,4-dicarboxylic acid di-*tert*-butyl ester [(9]aneN₃)(BOC)₂¹ (0.35 g, 1.06 mmol) in toluene (25 mL) was added KOH (0.18 g, 3.21 mmol) at room temperature under nitrogen. To this mixture was added **2** (0.25 g, 0.53 mmol) in dry CHCl₃ (10 mL) during 10 min. The mixture was stirred at 70 °C for 6 h and at room temperature for 24 h, filtered and concentrated under reduced pressure to give a yellow solid (0.48 g, 94% yield). M.p. 115°C. Elem. Anal. found. (calcd for C₅₄H₇₆N₆O₁₀): C, 66.4 (66.9); H, 7.5 (7.9); N 8.5 (8.7) %. ¹H-NMR (400MHz, CDCl₃), δ_H (ppm): 1.41 (s, 36H, CH₃(*t*-Bu)), 2.85-3.20 (m, 24H, [9]aneN₃ ring), 4.13 (s, 4H, ArCH₂N), 7.07-7.15 (m, 4H), 7.56 (s, 2H), 7.67 (d, 4H, J = 8.4 Hz). ¹³C-NMR (100MHz, CDCl₃), δ_C (ppm): 27.8, 28.2 (C(CH₃)₃), 46.9, 47.3, 47.7, 47.8, 49.2, 49.5, 50.1, 51.3, 52.0, 52.1, 52.7 ([9]aneN₃ ring), 59.8 (ArCH₂N), 79.6, 79.9 (C(CH₃)₃), 116.3, 122.3, 124.6, 124.9, 125.4, 127.1, 127.9, 128.7, 133.9, 155.3 (aromatic carbons), 153.1 (C=O).

Synthesis of L. To a solution of (BOC)₄-L (0.45 g, 0.46 mmol) in CH₂Cl₂ (10 mL) was added CF₃CO₂H (10 mL), and the resulting solution was stirred at room temperature under nitrogen for 2 h, then the solvent was removed under reduced pressure. The residue taken up in water, the pH value was adjusted to 9-10 by adding 1M NaOH, and the product extracted into CHCl₃ (4 x 20 mL). The organic layers were dried over Na₂SO₄, filtered and concentrated under vacuum to give a yellow solid (0.23 g, 88% yield). M.p. 135°C. Elem. Anal. found. (calcd for C₃₄H₄₄N₆O₂): C, 71.5 (71.8); H, 7.5 (7.8); N 14.4 (14.8) %. ¹H-NMR (400 MHz, CDCl₃), δ_H (ppm): 2.60-2.90 (m, 24H, [9]aneN₃ ring), 3.96 (s, 4H, ArCH₂N), 7.08-7.16 (m, 4H), 7.61 (s, 2H), 7.73 (d, 4H, J = 8.4 Hz). ¹³C-NMR (100MHz, CDCl₃) δ_C (ppm): 46.4, 47.0, 52.7 ([9]aneN₃ ring), 60.3 (ArCH₂N), 116.9, 122.5, 124.9, 125.7, 127.6, 127.9, 128.5, 134.4, 154.9 (aromatic carbons).



Scheme S1. Sketch of the synthetic procedure

Molecular modelling.

The starting 3D framework of the receptor was obtained by assembling appropriate molecular fragments ((*S*)-Binol and [9]aneN₃) retrieved from the Cambridge Structural Database (CSD; v 5.28).³ The acidic protons in (H₂L)²⁺ were localised on a secondary amine groups of each macrocyclic units, in keeping with their higher basicity with respect to tertiary ones. The starting model, roughly improved by an energy minimization procedure, underwent molecular dynamics (MD) simulations (time step = 1 fs, equilibration time = 100 ps, production time = 1000 ps, T = 300 K) in order to explore its potential energy surface in water, the latter simulated by using a distance dependent dielectric constant. Then energy minimization procedures (by using the steepest descent and conjugate gradient algorithms) was applied to obtain the final geometry of the diprotonated receptor. The programs used for the MD and the energy minimization were the simulation protocols Standard Dynamics Cascade and Minimization implemented in Accelrys Discovery Studio 1.7.⁴ The force field used in the simulation was CHARMM.⁵

Potentiometric measurements

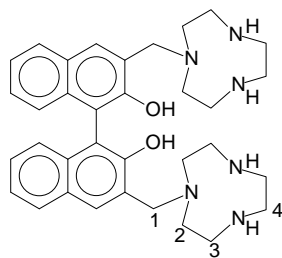
Equilibrium constants for protonation and complexation reactions were determined by means of potentiometric measurements (pH = -log [H⁺]), carried out in 0.1 M NMe₄Cl at 298.1 ± 0.1 K, in the pH range 2.5-10.5, by using the equipment that has been already described.⁶ The reference electrode was an Ag/AgCl electrode in saturated KCl solution. The glass electrode was calibrated as a hydrogen concentration probe by titrating known amounts of HCl with CO₂-free NaOH solutions

and determining the equivalent point by the Gran's method.⁷ This allow one to determine the standard potential E° , and the ionic product of water ($pK_w = 13.83 \pm 0.01$). 1×10^{-3} M ligand concentrations was generally employed in the potentiometric measurements. In the measurements with anions, the anion to ligand molar ratio was varied from 1 to 10:1. The sodium salts of the different anions were used in the titrations to evaluate the anion binding ability of the receptor. The computer program HYPERQUAD⁸ was used to calculate the protonation constants of the ligands (Table S1) and the stability constants of its complexes (Table S2) of the complexes from e.m.f. data. At least three measurements (about 100 experimental points each one) were performed for each system. The titration curves for each system were treated either as a single set or as separated entities without significant variations in the values of the protonation or complexation constants.

¹H NMR measurements.

¹H NMR spectra in D₂O solution at pH 7 were recorded at 298 K on a Bruker Avance 400 MHz instrument. Peak positions are reported relative to HOD at 4.75 ppm. The pH was calculated from the measured pD value by using the relationship $pH = pD - 0.40$.⁹

¹H NMR titrations were performed by addition of a solution 0.1 M of the anionic substrates to a solution 5×10^{-3} M of the receptor in aqueous solution buffered at pH 7 (TRIS buffer 0.1 M). All titrations were performed in 5 mm NMR tubes using Hamilton microsyringes. At pH 7, the aliphatic section of the ligand displays a set of four signals (two multiplets at 3.04 and 3.25 ppm, attributable to the methylene groups 2 and 3, a singlet at 3.38 ppm, attributable to the methylene group 1 and a doublet at 4.02 ppm for the methylene 4, see Scheme S1 for labelling). All these signals display downfield shifts upon addition of the different anions and achieve a constant value of the chemical shift in the presence of an excess of each anion, e. g., at complete complexation of the anion in solution. The stability constants of the complexes were obtained by monitoring the shifts observed for the aliphatic signals 1-4 of the receptor upon addition of the substrates. Each titration was repeated at least twice. Elaboration of the data points with the program HYPNMR,¹⁰ affords the formation constants reported in Table S3. The complexation-induced ¹H NMR chemical shifts (CIS, ppm), given in Table S4, were measured as the difference $\delta_{OBS} - \delta_L$ where δ_{OBS} is the chemical shift of a signal determined in D₂O solutions for complete formation of the complex and δ_L is the chemical shift of receptor signal in the absence of the anionic substrate.¹¹ The signals of the BINOL unit are partially superimposed e display minor shifts in the presence of the anionic substrates at this pH.



Scheme S1. Signals monitored in the ^1H NMR measurements

Spectrophotometric and Spectrofluorimetric Measurements

Absorption spectra were recorded on a Perkin-Elmer Lambda 25 spectrophotometer. Fluorescence emission spectra were collected on a Perkin Elmer LS55 spectrofluorimeter. In the measurements carried out at different pH values, HCl and NMe_4OH were used to adjust the pH values which were measured on a Metrohm 713 pH meter. TRIS buffer (5 mM) was used in the experiments performed at pH 7. In the fluorescence emission measurements, the bisnaphthol unit of L was excited at 279 nm.

CD Measurements. The CD spectra were recorded with a JASCO J-815 spectrometer (Jasco, Tokyo, Japan) at 20 °C in a 1 cm cell. The stock solutions were prepared by weighting compound into volumetric flask and diluting with UV-grade solvents. The CD spectra were measured in millidegrees and normalized into $\Delta\epsilon_{\text{max}} [1 \text{ mol}^{-1} \text{ cm}^{-1}]/\lambda[\text{nm}]$ units.

1. S. Kimura, E. Bill, E. Bothe, T. Weyhermüller, K. Wieghardt, *J. Am. Chem. Soc.*, 2001, **123**, 6025.
2. (a) R. C. Hegelson, S. C. Peacock, L. J. Kaplan, L. A. Domeier, P. Moreau, K. Koga, J. M. Mayer, Y. Chao, M. G. Siegel, D. H. Hoffman, G. D. Y. Sogah, *J. Org. Chem.* 1978, **43**, 1930. (b) M. Asakawa, P. R. Ashton, S. E. Boyd, C. L. Brown, S. Menzer, D. Pasini, J. F. Stoddart, M. S. Tolley, A. J. P. White, D. J. Williams, P. G. Wyatt, *Chem. Eur. J.* 1997, **3**, 463.
3. F. H. Allen, R. Taylor, *Chem. Soc. Rev.*, 2004, **33**, 463.
4. Accelrys.inc, San Diego California, USA
5. P. Swaminathan, M. Sundaralingam, *Acta Cryst Sect. B*, 1980, **36**, 2590. b) A.C. Larson, *Acta Cryst Sect. B*, 1978, **34**, 3601-3604.

6. S. Bartoli, C. Bazzicalupi, S. Biagini, L. Borsari, A. Bencini, E. Faggi, C. Giorgi, C. Sangregorio, and B. Valtancoli, *Dalton Trans.*, 2009, 1223.
7. G. Gran, *Analyst* 1952, 77, 661; F. J. Rossotti, H. Rossotti. *J. Chem. Educ.* 1965, **42**, 375.
8. P. Gans, A. Sabatini, A. Vacca, *J. Chem. Soc., Dalton Trans.* 1985, 1195.
9. A. K. Covington, M. Paabo, R. A. Robinson, R. G. Bates, *Anal. Chem.*, 1968, **40**, 700.
10. C. Frassinetti, S. Ghelli, P. Gans, A. Sabatini, M. S. Moruzzi and A. Vacca, *Anal. Biochem.*, 1995, **231**, 374-382.
11. C. Bazzicalupi, A. Bencini, C. Giorgi, B. Valtancoli, V. Lippolis, A. Perra *Inorg. Chem.*, 2011, **50**, 7202.

Table S1. Protonation constants of **L** determined by potentiometric measurements in 0.1 M NMe₄Cl at 298 K.

Reaction	Log K
$L + H^+ = HL^+$	10.53(4)
$HL^+ + H^+ = H_2L^{2+}$	8.42(4)
$H_2L^{2+} + H^+ = H_3L^{3+}$	5.20(4)
$H_3L^{3+} + H^+ = H_4L^{4+}$	2.79(6)
$H_4L^{4+} + H^+ = H_5L^{5+}$	2.6(1)

Table S2. Formation constants of the complexes determined by potentiometric measurements in 0.1 M NMe₄Cl at 298 K.

	(<i>S,S</i>)-tartaric ac.	(<i>R,R</i>)-tartaric ac.	<i>meso</i> -tartaric ac.	(<i>R</i>)-malic ac.
$H_2L^{2+} + A^{2-} = H_2LA$	5.8(1)	3.3(1)	3.8(1)	4.4(1)
$H_2L^{2+} + HA^- = H_3LA^+$	4.9(1)	2.4(1)	3.2(1)	3.7(1)
$H_3L^{2+} + HA^- = H_4LA^{2+}$	4.8(1)	2.6(1)	3.6(1)	3.8(1)
	(<i>S</i>)-malic ac.	succinic ac.	maleic ac.	fumaric ac.
$H_2L^{2+} + A^{2-} = H_2LA$	3.2(1)	3.5(1)	3.8(1)	2.7(1)
$H_2L^{2+} + HA^- = H_3LA^+$	2.9(1)	3.2(1)	3.0(1)	-----
$H_3L^{2+} + HA^- = H_4LA^{2+}$	3.0(1)	3.4(1)	3.3(1)	2.4(1)

Table S3. Formation constants of the complexes determined by ^1H NMR measurements at pH 7 (TRIS Buffer 0.1 M) at 298 K.

substrate	Log K
(<i>S,S</i>)-tartaric acid	6.1(1)
(<i>R,R</i>)-tartaric acid	2.5(1)
<i>meso</i> -tartaric acid	3.1(1)
(<i>R</i>)-malic acid	4.8(1)
(<i>S</i>)-malic acid	3.0(1)
succinic acid	3.7(1)
maleic acid	3.9(1)
fumaric acid	2.8(1)

Table S4. ¹H NMR chemical shifts for the aliphatic methylene groups 1, 2 3 and 4 of L in their adducts with the anions and corresponding chemical shift determined for complete substrate coordination (complexation-induced chemical shifts (CIS), ppm) measured in D₂O solution at pH 7.0 and 298 K.

Substrate	signal	H1	H2	H3	H4
<i>(S,S)</i> -tartrate	δ _{OBS}	3.87	3.66	3.30	4.25
	CIS ^a	0.49	0.41	0.25	0.25
<i>(R,R)</i> -tartrate	δ _{OBS}	3.70	3.52	3.16	4.12
	CIS	0.32	0.27	0.12	0.10
<i>meso</i> -tartrate	δ _{OBS}	3.68	3.56	3.18	4.14
	CIS	0.30	0.31	0.14	0.12
<i>(R)</i> -malate	δ _{OBS}	3.77	3.60	3.16	4.13
	CIS	0.39	0.35	0.12	0.11
<i>(S)</i> -malate	δ _{OBS}	3.68	3.53	3.27	4.15
	CIS	0.30	0.28	0.13	0.13
succinate	δ _{OBS}	3.70	3.54	3.11	4.07
	CIS	0.32	0.29	0.05	0.05
maleate	δ _{OBS}	3.71	3.52	3.11	4.08
	CIS	0.33	0.27	0.07	0.06
fumarate	δ _{OBS}	3.53	3.41	3.08	4.05
	CIS	0.15	0.16	0.04	0.03

^a The complexation-induced ¹H NMR chemical shifts (CIS, ppm) were measured as the difference δ_{OBS} – δ_L where δ_{OBS} is the chemical shift of a signal determined in D₂O solutions for complete formation of the complex and δ_L is the chemical shift of the resonance of receptor L in the absence of the anionic substrate.

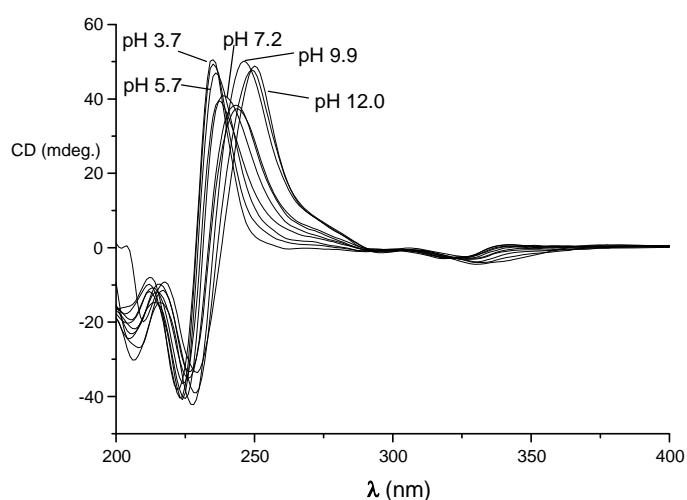


Figure S1. CD spectra of **L** at different pH values ($[L] = 3 \times 10^{-5} \text{ M}$).

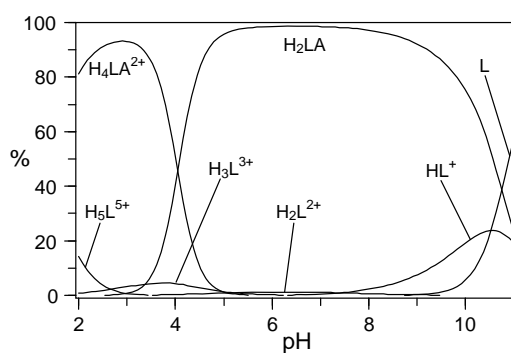


Figure S2. Distribution diagram of the complexes with (*S,S*)-tartaric acid ($[L] = [(S,S)\text{-tartaric acid}] = 1 \times 10^{-3} \text{ M}$)

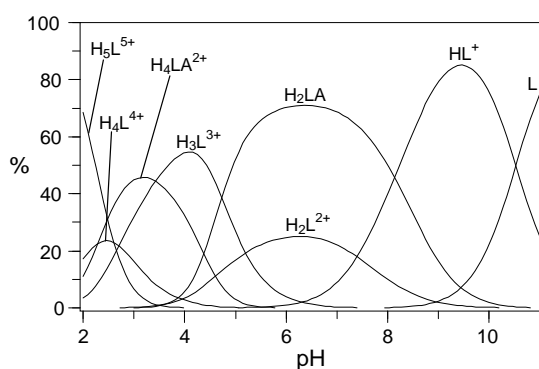


Figure S3. Distribution diagram of the complexes with (*R,R*)-tartaric acid ($[L] = [(R,R)\text{-tartaric acid}] = 1 \times 10^{-3} \text{ M}$)

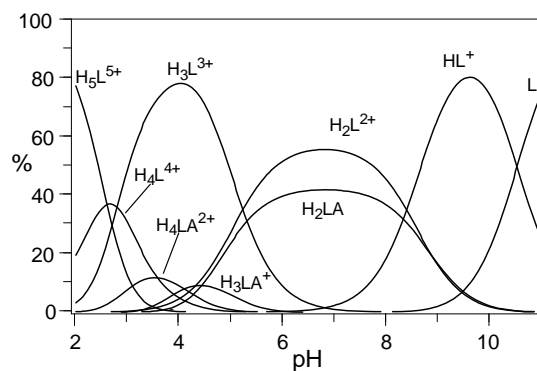


Figure S4. Distribution diagram of the complexes with *meso*-tartaric acid ($[L] = [(meso)\text{-tartaric acid}] = 1 \times 10^{-3} \text{ M}$)

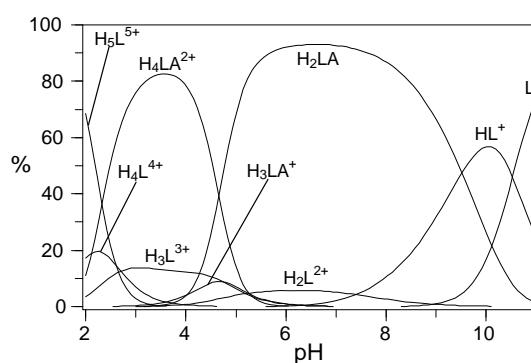


Figure S5. Distribution diagram of the complexes with (*R*)-malic acid ($[L] = [(R)\text{-malic acid}] = 1 \times 10^{-3} \text{ M}$)

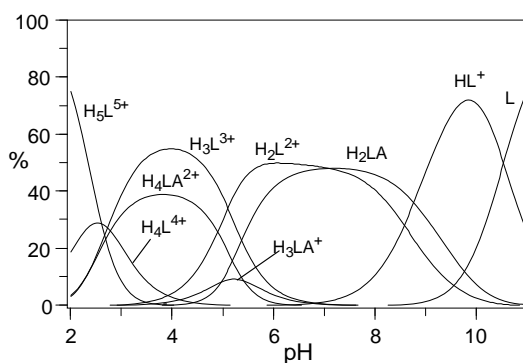


Figure S6. Distribution diagram of the complexes with (*S*)-malic acid ($[L] = [(S)\text{-malic acid}] = 1 \times 10^{-3} \text{ M}$)

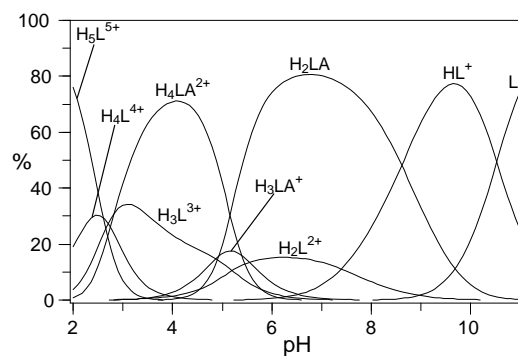


Figure S7. Distribution diagram of the complexes with succinic acid ($[L] = [\text{succinic acid}] = 1 \times 10^{-3} \text{ M}$).

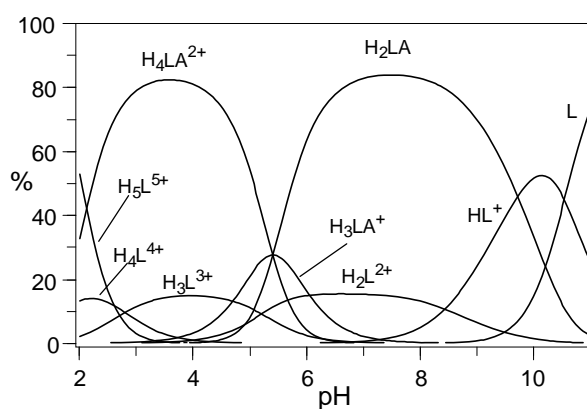


Figure S8. Distribution diagram of the complexes with maleic acid ($[L] = [\text{maleic acid}] = 1 \times 10^{-3} \text{ M}$).

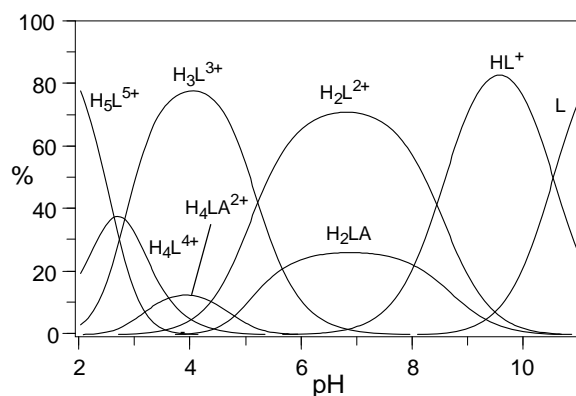


Figure S9. Distribution diagram of the complexes with fumaric acid ($[L] = [\text{fumaric acid}] = 1 \times 10^{-3} \text{ M}$).

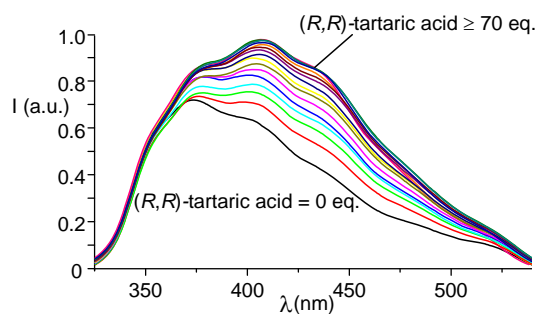


Figure S10. Fluorescence emission spectra of **L** at pH 7 and 298 K in the presence of increasing amounts (5 eq. each addition) of (R,R) -tartaric acid. ($[L] = 3 \cdot 10^{-5}$, $\lambda_{exc} = 279$ nm)

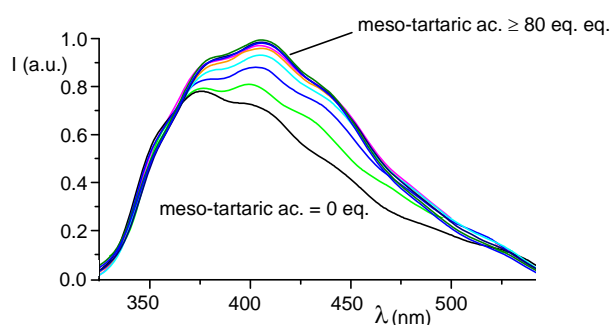


Figure S11. Fluorescence emission spectra of **L** at pH 7 and 298 K in the presence of increasing amounts (10 eq. each addition) of *meso*-tartaric acid. ($[L] = 3 \cdot 10^{-5}$, $\lambda_{exc} = 279$ nm).

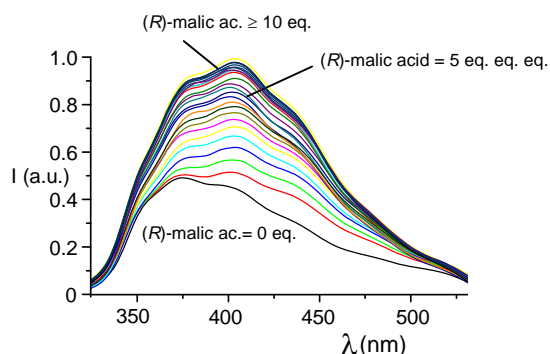


Figure S12. Fluorescence emission spectra of **L** at pH 7 and 298 K in the presence of increasing amounts (0.5 eq. each addition) of (R) -malic acid. ($[L] = 3 \cdot 10^{-5}$, $\lambda_{exc} = 279$ nm).

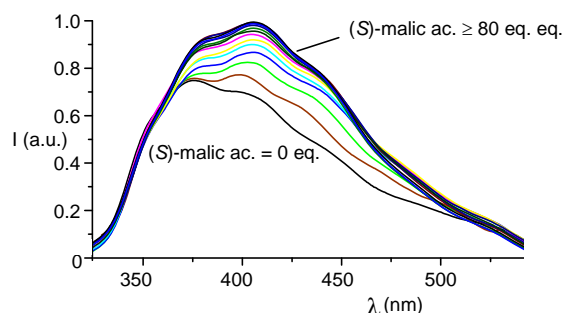


Figure S13. Fluorescence emission spectra of **L** at pH 7 and 298 K in the presence of increasing amounts (10 eq. each addition) of (*S*)-malic acid ($[L] = 3 \cdot 10^{-5}$, $\lambda_{\text{exc}} = 279$ nm).

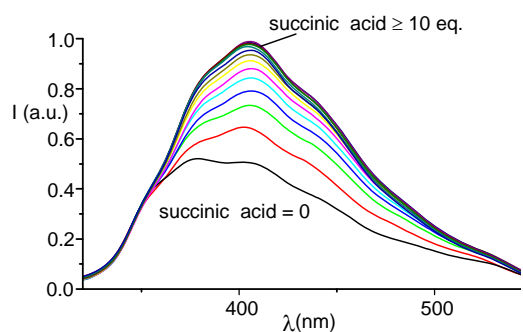


Figure S14. Fluorescence emission spectra of **L** at pH 7 and 298 K in the presence of increasing amounts (1 eq. each addition) of succinic acid ($[L] = 3 \cdot 10^{-5}$, $\lambda_{\text{exc}} = 279$ nm).

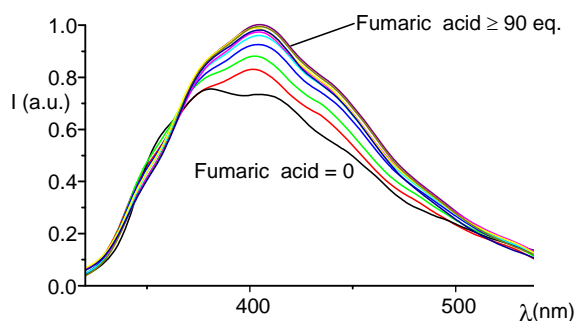


Figure S15. Fluorescence emission spectra of **L** at pH 7 and 298 K in the presence of increasing amounts (10 eq. each addition) of fumaric acid ($[L] = 3 \cdot 10^{-5}$, $\lambda_{\text{exc}} = 279$ nm).

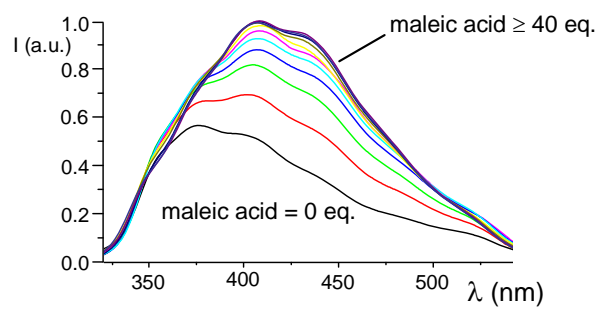


Figure S16. Fluorescence emission spectra of **L** at pH 7 and 298 K in the presence of increasing amounts (5 eq. each addition) of maleic acid ($[L] = 3 \cdot 10^{-5}$, $\lambda_{\text{exc}} = 279$ nm).